J|A|C|S
A R T I C L E S

Conformational Analysis of a Stereochemically Complete Set of Cis-enediol Peptide Analogues

Olivier Michielin,[†] Vincent Zoete,[†] Tiffany Malinky Gierasch,[‡] Jens Eckstein,[§] Andrew Napper,[§] Gregory Verdine,[‡] and Martin Karplus[*,†,‡]

Contribution from the Laboratoire de Chimie Biophysique Institut Le Bel, Université Louis Pasteur, 4 rue Blaise Pascal, 67000 Strasbourg, France, Department of Chemistry and Chemical Biology, Harvard University, 12 Oxford Street, Cambridge, Massachusetts 02138, and Enanta Pharmaceuticals, 500 Arsenal Street, Watertown, Massachusetts

Abstract: A conformational analysis of a stereochemically complete set of peptide analogues based on a cis-enediol unit is presented. The cis-enediol unit, which can replace a two or a three amino acid segment of a peptide, contains two "side chains", four asymmetrical carbon atoms, and six free dihedral angles. To determine the accessible conformational space, the molecules are divided into three fragments, each containing two free dihedral angles. The energy surfaces are computed for all dihedral angle values, and the possible conformations of the cis-enediol unit analogues are built using all combinations of the surface minima. Such a "build-up" procedure, which is very fast, is able to reproduce 75% of the minima obtained from a full dihedral angle exploration of the conformational space. The cis-enediol unit minima are compared with the corresponding di- and tripeptide minima; all peptide minima can be closely matched by a cis-enediol unit minimum of low energy (less than 2.2 kcal/mol above the lowest energy conformer). However, there are low energy minima of the cis-enediol unit that have no corresponding minima in peptides. The results are shown to depend strongly on the chirality of the analogues. The ability of each of the stereoisomers to mimic natural peptides, evaluated by the present approach, is correlated with its experimental activity in a renin inhibition assay.

1. Introduction

Peptide analogues are important drug design tools because of their abilities to act as substitutes for peptides in active sites of enzymes and receptors.[1] Here we report an analysis of the conformational properties of a new family of peptide analogues, whose synthesis has been described recently.[2] The analogues are based on a cis-enediol unit (CPEP, see Figure 1) containing two "side chains", four asymmetrical carbon atoms, and six free dihedral angles. There exist 16 different stereoisomers composed of 8 pairs of enantiomers, see Figure 1. Most peptidomimetics are designed to reproduce natural peptides as closely as possible. The present set is introduced to have a conformation space that includes regions that are both similar to and different from those of natural peptides. Moreover, the existence of a large number of stereoisomers introduces possible specificities not available in peptides.

The peptide analogues described here can mimic either a two or a three amino acid segment of a peptide. The presence of a

C−C double bond makes them resistant to protease degradation,[2] and contributes to a less polar backbone, which may allow better cellular membrane penetration. The analogues can be inserted in the middle of a regular peptide sequence and different side chains can be substituted for the methyl groups to mimic the natural ligands of important targets, such as HIV-1 protease or MHC Class I molecules.

The aim of the present study is to examine the energy surfaces of the peptide analogues by different approaches, including a thorough dihedral-angle grid-scan search, a rapid construction or "build-up"[3] procedure based on dipeptide fragments and molecular dynamics (MD) simulations. These methods are tested and compared to evaluate them for future drug design applications and folding studies involving larger molecules for which a complete grid search is prohibitive. The results of the conformational space analysis are compared with those for natural peptides.

Section 2 describes the methods used. The determination of the force field parameters for the peptide analogues is presented, followed by a description of the various approaches employed to sample the conformational space. A brief description of the experimental methods used for measuring the binding to renin is given. Section 3 gives the results obtained from each of the search methods. The ability of each of the stereoisomers to

* To whom correspondence should be addressed. E-mail: marci@tammy.harvard.edu.
† Université Louis Pasteur.
‡ Harvard University.
§ Enanta Pharmaceuticals.

(1) Kieber-Emmons, T.; Murali, R.; Greene, M. *Curr. Opin. Biotechnol.* **1997**, *8*, 435−441.
(2) Gierasch, T. M.; Chytil, M.; Didiuk, M. T.; Park, J. Y.; Urban, J. J.; Nolan, S. P.; Verdine, G. *Org. Lett.* **2000**, *2*, 3999−4002.
(3) Vasquez, M.; Scheraga, H. *J. Biomol. Struct. Dyn.* **1988**, *5*, 705−755.
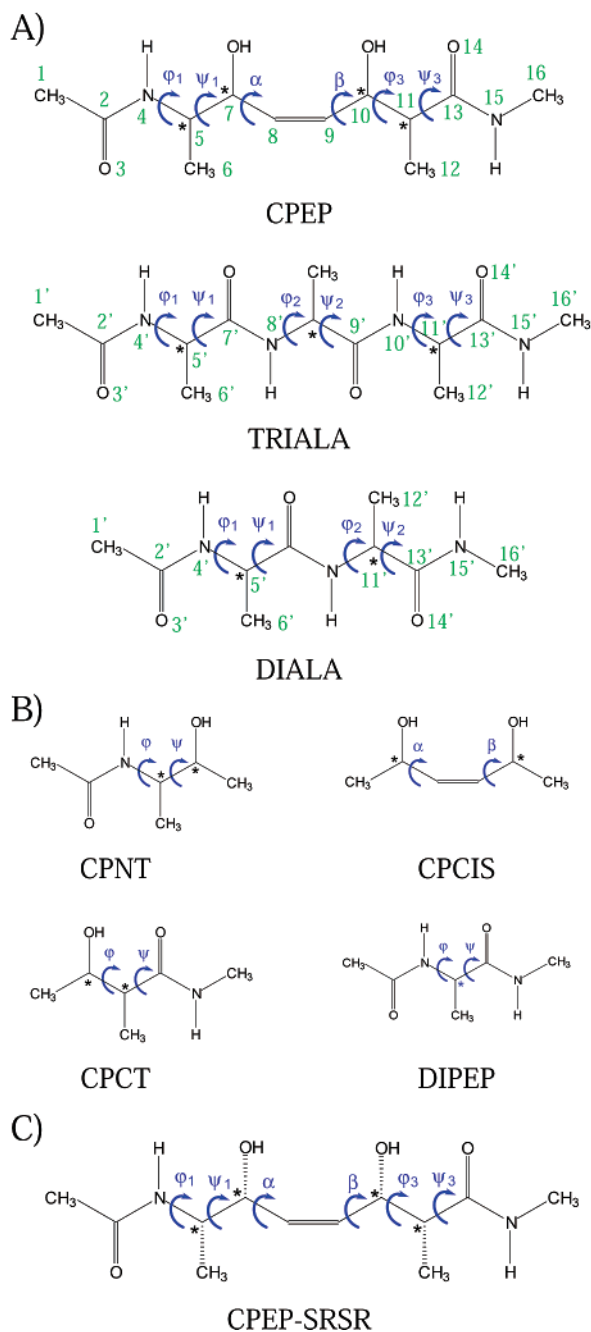
Figure 1. (A) Generic structure of peptide analogues: The family of peptide analogues is characterized by a C—C double bond replacing the usual peptidic bond. Various groups can be substituted for the methyl groups: isopropyl, isobutyl, benzyl, etc. The molecule contains six free dihedral angles: ϕ_1/ψ_1, α/β, and ϕ_3/ψ_3. The four asymmetrical carbon atoms are indicated; all R/S configurations are possible to synthesize, but the C—C double bond must be in the Z configuration. Only eight configurations needed to be studied because there are eight pairs of enantiomers; in an asymmetric environment (i.e., a protein ligand), they behave differently. The structure of the alanine dipeptide and tripeptide used for comparison is shown below; the green numbers indicate the correspondence used to superimpose the analogue. (B) Structure of the fragments used to compute the maps: CPNT, CPCT, and CPCIS are the N-terminal, the C-terminal, and the central part of the cis-enediol peptide (CPEP), respectively. For the TRIALA and DIALA maps, two or three DIPEP units were used. (C) Configurations of the asymmetrical carbons of SRSR CPEP.

mimic natural peptides is compared with the experimental data on their binding to renin. Section 4 presents the conclusions.

2. Methods

2.1. Parameters Determination. The conformation space of the peptide analogues was sampled by use of the CHARMM program.[4] Because the peptide analogues involve nonstandard residues, force field parameters consistent with the existing CHARMM force field[5] needed to be developed. As a starting point, the Merck molecular force field (MMFF),[6] which generated the necessary parameters, was used to determine the minimum energy conformation of the RRRR CPEP shown in Figure 1A. The resulting structure was used as a starting point for a Hartree−Fock/6-31G* ab initio calculation using the GAMESS[7] program to find the optimum structure. Partial charges centered on the nuclei were determined by fitting the electrostatic potential derived from the ab initio calculation, using a program based on a least-squares algorithm and applying constraints to ensure that symmetrical atoms have the same partial charges. The atomic partial charges of the CPEP molecule are provided in the Supporting Information. Force constants were obtained from the second derivative of the Hartree−Fock/6-31G* energy surface (Hessian matrix) with respect to the internal coordinates. The van der Waals parameters were taken from existing CHARMM atom types; the closest existing CHARMM atom type was chosen on the basis of electronic structure similarity.

2.2. Conformation Space Search. Several methods were used to sample the conformational space of the peptide analogues. A thorough exploration was performed using a grid-scan procedure with the eight different stereoisomers having methyl groups on the "C_α" positions, as depicted in Figure 1. A quick construction method (build-up procedure) using the lowest energy regions of the dihedral angle energy surfaces of fragments was also tested. Finally, the conformational space was sampled using MD simulations at various temperatures.

2.2.1. Grid Scan. Each of the six dihedrals ϕ_1/ψ_1, ϕ_2/ψ_2 (α/β for CPEP), and ϕ_3/ψ_3 were varied by 60° intervals. The resulting $6^6 = 46\,656$ conformations were minimized using the protocol shown in Figure 2. Starting from the Hartree−Fock 6-31G* Cartesian coordinates, we built the internal coordinate (IC) table and assigned the new values for the six dihedral angles. The Cartesian coordinates were reconstructed and submitted to a short 200 steps steepest descent energy minimization to remove clashes arising from the change in dihedral values. The dihedral angles were constrained during this step by applying a harmonic potential of 100 kcal/mol/rad[2]. To complete the minimization, the dihedral constraints were removed, and the adopted basis Newton−Raphson method (ABNR) in the CHARMM program was used to reduce the energy gradient to less than 10^{-2} kcal/(mol Å). To proceed to the next geometry, the IC table was recomputed from the Cartesian coordinates of the previous minimization, and the new values for the dihedrals were assigned. Thus, the previous geometry was used as a preconditioner, improving significantly the convergence time of the minimization. All minimizations and energy evaluations were made using a distance independent dielectric constant of $\epsilon = 80$, using a shifted electrostatic energy term and a cutoff of 12 Å. The final conformation was stored together with the total, bonded, electrostatic, and van der Waals energy terms. The "solution" value ($\epsilon = 80$) was used for the dielectric constant to lower the contribution of the electrostatic interactions to the total energy surface, which is thus mainly determined by the bonded and van der Waals terms.

(4) Brooks, B. R.; Bruccoleri, R. E.; Olafson, B. D.; States, D. J.; Swaminathan, S.; Karplus, M. *J. Comput. Chem.* **1983**, *4*, 187−217.
(5) MacKerell, A. D.; Bashford, D.; Bellott, M.; Dunbrack, R.; Evanseck, J.; Field, M.; Fischer, S.; Gao, J.; Guo, H.; Ha, S.; Joseph-McCarthy, D.; Kuchnir, L.; Kuczera, K.; Lau, F.; Mattos, C.; Michnick, S.; Ngo, T.; Nguyen, D.; Prodhom, B.; III, W. R.; Roux, B.; Schlenkrich, M.; Smith, J.; Stote, R.; Straub, J.; Watanabe, M.; Wiorkiewicz-Kuczera, J.; Yin, D.; Karplus, M. *J. Phys. Chem. B* **1998**, *102*, 3586−3616.
(6) Halgren, T. A. *J. Comput. Chem.* **1996**, *17*, 490−519.
(7) Schmidt, M. W.; Baldridge, K. K.; Boatz, J. A.; Elbert, S. T.; Gordon, M. S.; Jensen, J. J.; Koseki, S.; Matsunaga, N.; Nguyen, K. A.; Su, S.; Windus, T. L.; Dupuis, M.; Montgomery, J. A. *J. Comput. Chem.* **1993**, *14*, 1347−1363.
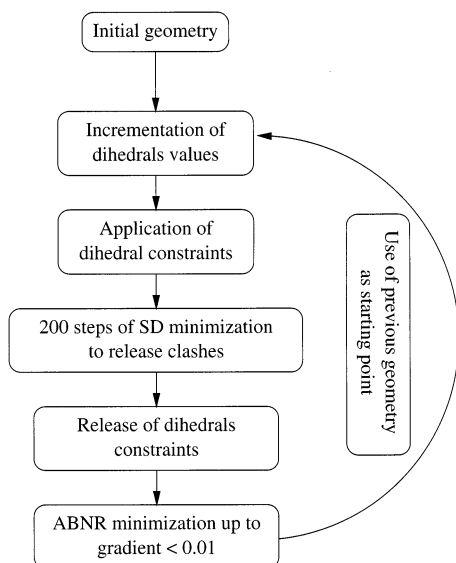
Figure 2. Minimization protocol for grid scan. At each step, new dihedral values were imposed to the geometry obtained from the previous minimization (used as a preconditioner) using a constraint of 100 kcal/mol/rad^2 for the first 200 steps of SD minimization. This prevented large deviations in the dihedral value due to clashes at the beginning of the minimization. The dihedral constraints were subsequently removed, and an unrestrained minimization was performed until a gradient of less than 0.01 kcal/(mol Å) was obtained. The use of the previous minimized geometry as a starting geometry for the next step improved greatly the convergence of the minimization.

The conformations generated by the grid-scan procedure were clustered to obtain a smaller set of conformers that would reliably represent the conformational space. The clustering was based on the dihedral angles values using a range of 30° summed over the six dihedrals, corresponding to an average deviation of 5° per dihedral in the cluster. The all-atom Cartesian RMSD matrix between all members of a given cluster was computed to check that all conformers clustered in dihedral space were also close in Cartesian space. A representative of each cluster was chosen by taking the conformer whose dihedral angle values were closest to the average values for the given cluster; its energy was used to define the energy of the cluster. Such a clustering procedure typically resulted in the identification of about 300 clusters for each stereoisomer, with a range of energies and sizes. To reduce the number of clusters even further, we excluded all clusters having an energy

$$E_{cl} > \alpha e^{\beta S_{cl}} \qquad (1)$$

where S_{cl} is the size of the cluster, α is the lowest energy in the ensemble of clusters found for the stereoisomer plus 5 kcal/mol, and β is chosen such that exactly 150 clusters are kept. In this way, the low energy and large size clusters were selected. The selection was not based on the energy alone, because the size of the cluster reflects the broadness of the basin of the local minimum which contributes to a higher probability for this state. The 150 selected clusters for each stereoisomer are included in a database available in the Supporting Information.

2.2.2. Rapid Build-Up Procedure. One approach to finding low energy conformers for larger peptides makes use of a build-up procedure.[3] Because a full grid-scan search is possible in the present case, it was of interest to test the build-up procedure by comparing the conformers obtained from it with those from the grid search. To predict the low energy conformations of the peptide analogues, maps were computed for the ϕ_1/ψ_1, α/β, and ϕ_3/ψ_3 dihedral angles. Energy surfaces were determined for minimal fragments of the analogue and the alanine peptide with the corresponding dihedral angles. For the peptide analogues, the following fragments were used: N-terminal fragment

(ϕ_1/ψ_1), extending from the N-terminus up to the first C of the double bond replaced by a methyl group, that is, 3-acetylamino-butanol-2 (CPNT, Figure 1); C-terminal fragment (ϕ_3/ψ_3), extending from the C-terminus up to the first C of the double bond replaced by a methyl group, that is, β-hydroxy-α-methyl-N-methylbutanamide (CPCT, Figure 1); central fragment (ϕ_2/ψ_2), containing the central C—C (CIS-configured) double bond and all of the atoms up to the C-terminal and N-terminal "Cα" atoms replaced by methyl groups, that is, Z-2,5-dihydroxy-hexene-3 (CPCIS, Figure 1). For the natural alanine peptide, the following fragment was used: central fragment (ϕ_2/ψ_2), extending from the N-terminus of DIALA up to the second Cα replaced by a methyl group, that is, α-(acetylamino)-N-methylpropanamide (DIPEP, Figure 1). The energy surfaces were obtained by varying the two dihedral angles at 10° increments to span the entire dihedral space. At each value, the structure was minimized using the ABNR method[4] with constraints of 1000 kcal/mol/rad^2 on the dihedral angles. At the end of the minimization, the van der Waals, electrostatic, bonded, and total energy contributions were evaluated for each conformer, not including the dihedral constraints. As before, a distance independent dielectric constant of 80 was used during minimization and for evaluation of the energy terms.

The construction of the peptide analogue map was based on the dihedral angle energy surfaces for the fragments. Six energy minima for the ϕ_1/ψ_1 surface, (−120,−60), (−120,60), (−120,170), (75,−75), (60,−65), and (75,165), four for the ϕ_2/ψ_2, (−120,−60), (−120,120), (60,120), and (120,−120), and six for the ϕ_3/ψ_3, (−165,−65), (−165,115), (−60,−60), (−60,120), (65,−65), and (65,115), were selected, and the 144 possible conformers were built and minimized as described for the grid-scan procedure, see section 2.2.1; the Cartesian coordinates were reconstructed and submitted to a short 200 steps steepest descent energy minimization to release clashes arising from the change in dihedral angle values. The dihedral angles were prevented from changing during this step by applying a quadratic constraint of 100 kcal/mol/rad^2. To complete the minimization, the dihedral constraints were removed, and the ABNR method was used to obtain energy gradients of less than 10^{-2} kcal/(mol Å).

2.2.3. Molecular Dynamics Simulations. As an alternative way to explore the conformational space, molecular dynamics simulations of the peptide analogues were made at three temperatures (400, 500, and 600 K). Starting from one of the cluster centers found in the grid-scan method ($\phi_1/\psi_1 = (−120.05,−58.55)$, $\phi_2/\psi_2 = (−159.42,166.57)$, and $\phi_3/\psi_3 = (−162.97,−65.69)$, energy 38.215 kcal/mol and population of 403 members), we heated the SRSR peptide analogue during 4, 5, and 6 ps, respectively, and equilibrated for 100 ps. The production run consisted of a 20 ns simulation. The integration time step was 1 fs. A distance independent dielectric constant of $\epsilon = 80$, with a shifted electrostatic energy term and a cutoff of 12 Å, was used.

The frames of the trajectory were clustered using the dihedral angle values and a radius of 30°, as described in section 2.2.1. No selection of the most representative clusters was needed because the total number of clusters was usually reasonably small (e.g., on the order of 150 or less).

2.2.4. Renin Inhibition Data. Sixteen stereoisomers, corresponding to a Z configuration of the double bond peptide analogues with two different sequences, were tested for inhibition of renin.

The sequence of the human angiotensinogen residues flanking the renin cleavage site is given by DRVYIHPFHL-VIHN, where L-V corresponds to the cleavage site. The peptide analogue libraries, of 16 stereoisomers each, were based on this peptide. The new molecules were designed to replace the scissile bond "L-V". The two libraries are as follows: (i, i + 1) peptide analogue, Ac-PHPFH"L-L"IHK-NH$_2$; (i, i + 2) peptide analogue, AC-PHPFH"L-L"HK-NH$_2$, with "L-L" = −NHCH(iBu)CH(OH)C═CCH(OH)CH(iBu)CO−, and iBu = CH$_2$CH-(CH$_3$)$_2$. Thus, the (i, i + 1) and (i, i + 2) libraries were designed as analogues of human angiotensinogen in which two amino acids (LV)

Table 1. Dipole Magnitudes (debyes) Computed for DIALA, TRIALA, and All of the CPEP Stereoisomers[a]

	stereoisomer	HF-6.31G* dipole[b]	average algebraic[c]	average Boltzmann[d]
CPEP	RRRR	5.93	6.51(2.45)	6.31
	RRRS	5.20	6.56(2.39)	6.21
	RRSR	5.00	6.62(2.44)	6.44
	RRSS	3.64	6.49(2.56)	6.55
	RSRR	3.33	6.76(2.54)	6.67
	RSRS	5.71	6.96(2.60)	6.82
	RSSR	1.74	6.68(2.54)	6.72
	RSSS	3.44	6.71(2.51)	6.71
	SRRR	3.43	6.69(2.51)	6.70
	SRRS	1.10	6.69(2.53)	6.63
	SRSR	5.71	6.90(2.67)	6.73
	SRSS	3.30	6.68(2.55)	6.76
	SSRR	6.33	6.38(2.56)	6.78
	SSRS	5.01	6.72(2.42)	6.75
	SSSR	5.16	6.57(2.39)	6.71
	SSSS	7.44	6.41(2.52)	6.70
average		4.47(1.65)	6.65(0.15)	6.64(0.17)
DIALA		11.29	7.28(3.34)	7.80
TRIALA		14.28	8.79(3.60)	12.41

[a] The dipoles were derived from the electronic density obtained from a single point Hartree−Fock/6-31G* calculation using the geometry of the lowest energy conformer for DIALA, TRIALA, and for each CPEP stereoisomer, or averaged over all of the minima included in the database using the partial charges determined in section 2.1. [b] Dipole magnitude computed from the HF-6.31G* electronic density using the geometry of the lowest energy conformer. [c] Algebraic average dipole magnitude computed from all of the minima included in the database. These results were obtained using the precomputed partial charges, see section 2.1; no ab initio calculations were performed. Standard deviations are given in parentheses. [d] Averaging as for [c] using Boltzmann weighting,

$$\langle P \rangle = \frac{\sum_i P_i e^{-\beta E_i}}{\sum_i e^{-\beta E_i}}$$

where i spans all of the conformations in the database.

or three amino acids (LVI) are replaced by the "L-L" linkage, respectively.

Inhibition of renin was tested using recombinant human renin in an enzymatic assay. Renin activity was measured using a fluorogenic angiotensinogen substrate from Molecular Probes (Eugene, OR). The assay is based on a previously described method.[8] Briefly, generation of the following fluorescent compound indicates activity of renin:

RE(EDANS)IHPFHL-VIHTK(DABCYL)R →
RE(EDANS)IHPFHL   (fluorescent)

Enzyme activity was determined from the rate of increase in fluorescence over 30 min at 37 °C. Inhibitory activity of library compounds was determined by competition against the fluorescent substrate. Plotting of the inhibition data resulted in sigmoidal curves with Hill slopes close to unity indicating one competition site. Inhibition of renin by the reference peptide Ac-PHPFHLLIHK-NH$_2$ representing the unmodified angiotensinogen sequence was determined in similar fashion; that is, the reference IC$_{50}$ refers to competition with the fluorescent substrate. IC$_{50}$ values were calculated from duplicate determinations of enzyme activity at a range of inhibitor concentrations. Fits to the data were obtained with GraphPad Prism (GraphPad Software,

(8) Holzman, T. F.; Chung, C. C.; Edalji, R.; Egan, D. A.; Martin, M.; Gubbins, E. J.; Krafft, G. A.; Wang, C. T.; Thomas, A. M.; et al. *J. Protein Chem.* **1991**, *10*, 553−563.

Table 2. Percentage of Trialanine Minima that Are Matched by Each Stereoisomer of CPEP with a Given RMSD Tolerance

isomer	RMSD tolerance (Å) 1.0	1.1	1.2
RRRR	47.97%	72.36%	89.43%
RRRS	44.72%	69.92%	91.87%
RRSR	57.72%	81.30%	93.50%
RRSS	28.46%	52.85%	81.30%
RSRR	49.59%	77.24%	96.75%
RSRS	34.96%	65.04%	91.06%
RSSR	59.35%	83.74%	95.12%
RSSS	36.59%	56.10%	86.18%
SRRR	70.73%	90.24%	98.37%
SRRS	66.67%	86.99%	99.19%
SRSR	87.80%	95.12%	100.00%
SRSS	69.11%	86.99%	100.00%
SSRR	77.24%	90.24%	97.56%
SSRS	59.35%	88.62%	97.56%
SSSR	83.74%	96.75%	99.19%
SSSS	52.03%	81.30%	98.37%

Table 3. Percentage of the 17 DIALA and 150 TRIALA Minima that Are Best Matched (Lowest RMSD) by a Given CPEP Stereoisomer

stereoisomer[a]	DIALA	TRIALA	stereoisomer[a]	DIALA	TRIALA
RRRR[(1)]	0.0	3.2	SSSS[(1')]	0.0	8.9
RRRS[(2)]	0.0	0.8	SSSR[(2')]	0.0	16.1
RRSR[(3)]	0.0	6.5	SSRS[(3')]	11.8	5.6
RRSS[(4)]	5.9	1.6	SSRR[(4')]	5.9	10.5
RSRR[(5)]	0.0	1.6	SRSS[(5')]	11.8	5.6
RSRS[(6)]	17.6	0.8	SRSR[(6')]	17.6	23.4
RSSR[(7)]	29.4	3.2	SRRS[(7')]	0.0	0.8
RSSS[(8)]	0.0	4.0	SRRR[(8')]	0.0	7.3

[a] Enantiomer pairs are indicated.

Table 4. Values of the Mean (μ) and Standard Deviation (σ) Obtained by Fitting a Gaussian to the RMSD Matrix Element Distribution Shown in Figure 9A

stereoisomer[a]	DIALA μ	DIALA σ	TRIALA μ	TRIALA σ
SRSR[(1)]	1.79501	0.435218	1.90325	0.430233
SSRR[(2)]	1.79589	0.441103	1.90404	0.433167
SRRR[(3)]	1.80674	0.437510	1.90969	0.449880
SSSR[(4)]	1.81151	0.429091	1.90282	0.435326
RRRR[(5)]	1.83302	0.379269	1.91337	0.418379
RSRR[(6)]	1.83641	0.400860	1.91835	0.418082
SRSS[(6')]	1.84064	0.394892	1.90626	0.422505
RRSR[(7)]	1.84394	0.394708	1.92183	0.422027
SSSS[(5')]	1.84433	0.374022	1.91085	0.407673
SSRS[(7')]	1.85091	0.383963	1.91433	0.410890
RSSR[(8)]	1.85266	0.414127	1.91179	0.421604
SRRS[(8')]	1.85277	0.395004	1.91221	0.428461
RSRS[(1')]	1.87896	0.362651	1.92248	0.411712
RSSS[(3')]	1.88220	0.360961	1.92853	0.403003
RRSS[(2')]	1.88558	0.360207	1.91931	0.396823
RRRS[(4')]	1.89646	0.367853	1.92242	0.422225

[a] Enantiomer pairs are indicated.

San Diego, CA) using the "sigmoidal dose-response, variable slope" equation:

$Y =$ bottom + (top − bottom)/
$$(1 + \exp((\log IC_{50} - X) \times \text{Hill slope}))$$

Standard deviations of determined IC$_{50}$ values are shown in brackets in Table 5.

3. Results and Discussion

3.1. Properties Related to Electronic Structure. The partial charges derived by fitting the electrostatic potential obtained

Table 5. Renin Inhibition Experimental Data for the (i, $i + 1$) and (i, $i + 2$) Peptide Analogues[a]

stereoisomer	matched tria.[b]	IC$_{50}$[c] (μM)	
		(i, $i + 1$)	(i, $i + 2$)
RRRR	47.97	1130(2.5)	409(3.5)
RRRS	44.72	340(1.4)	990(22.2)
RRSR	57.72	>1000	>1000
RRSS	28.46	>1000	135(1.3)
RSRR	49.59	>1000	>1000
RSRS	34.96	767(2.1)	>1000
RSSR	59.35	168(1.2)	319(1.7)
RSSS	36.59	1110(5.6)	216(1.6)
SRRR	70.73	11.3(1.2)	11.7(1.3)
SRRS	66.67	11.1(1.3)	109(1.2)
SRSR	87.80	15.2(1.4)	181(1.3)
SRSS	69.11	215(1.4)	305(2.5)
SSRR	77.24	46.6(1.4)	31.9(1.4)
SSRS	59.35	21.1(1.3)	159(1.3)
SSSR	83.74	13.2(1.1)	63(1.4)
SSSS	52.03	10.2(1.4)	131(1.9)
Ac−PHPFHLLIHK−NH2		405(1.3)	

[a] The activity of the reference peptide is also reported. Standard deviations of determined IC$_{50}$ are given in parentheses. These data are properties of Enanta Pharmaceuticals, Inc. [b] Percentage of trialanine minima that are matched by each stereoisomer of CPEP with an RMSD tolerance of 1.0 Å. [c] Renin inhibition activity of the peptide analogues.

from the Hartree−Fock/6-31G* electronic density are given in the Supporting Information. To compare the electronic properties of the various stereoisomers of the peptide analogue with the DIALA and TRIALA, a single point Hartree−Fock/6-31G* ab initio calculation using GAMESS[7] was performed for the minimum energy conformation obtained from the grid-scan procedure for DIALA, TRIALA, and the different CPEP stereoisomers, see section 2.1. Dipole moments were computed from the electron density, and the results are given in the first column of Table 1. The magnitudes of the dipolar moments are quite variable from one stereoisomer to another, ranging from 1.1 D for the SRRS stereoisomer up to 7.4 D for the SSSS. However, these values are still lower than their counterparts for standard peptides, with values of 11.3 D for DIALA and 14.3 D for TRIALA. The difference is due to the polar peptide bond. In the low energy DIALA and TRIALA conformations, the peptide bonds are pointing in the same direction, leading to a strong negative potential due to the dipole moment of the carbonyl groups. The dipole moments of two and three peptide bonds are added together in the lowest energy conformer of DIALA and TRIALA, respectively, whereas in the lowest energy conformer of CPEP, the cis-enediol unit does not contribute significantly to the dipole moments. Because these results are dependent on the conformation, the dipole moments were also computed for the entire DIALA, TRIALA, and CPEP sets of minima using the partial charges developed in the force field section, see section 2.1. The algebraic and Boltzmann weighted averages are very similar for the different stereoisomers. The cis-enediol unit appears to be significantly less polar than regular di- or tripeptides as judged by the Boltzmann weighted average of 7.80 and 12.41 D for DIALA and TRIALA, respectively, as compared to an average of 6.64($\pm$0.17) for all of the CPEP stereoisomers (see Table 1). These results show that the dipole moment expectation value is lower for CPEP than that of regular peptides, in accord with the results obtained for the lowest energy conformers alone.

3.2. Exploration of the Conformation Space. In the following sections, we present the results obtained with the
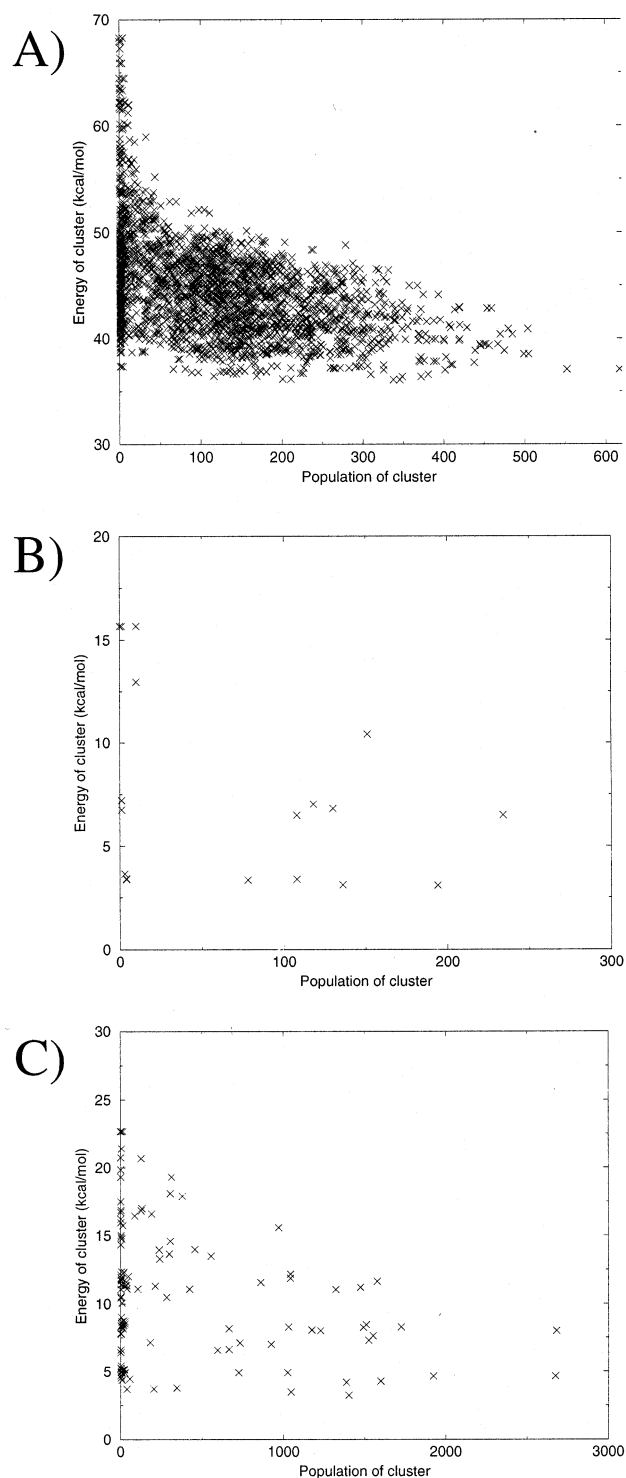

Figure 3. Clustering of the minima obtained by the grid-scan procedure with $\epsilon = 80$ for (A) the eight stereoisomers of CPEP (around 300 clusters for each stereoisomer), (B) DIALA (17 clusters), and (C) the TRIALA (124 clusters).

various methods used to search the conformational space. To aid in the interpretation of these results, the dihedral angle energy surfaces for the fragments used in the build-up procedure are described first.

3.2.1. Fragment Dihedral Angle Energy Surfaces. The dihedral angle energy surfaces are shown in Figure 4 for DIPEP and in Figure 5A for CPNT, CPCIS, and CPCT. The maps for the CPNT (ϕ_1/ψ_1) and CPCT (ϕ_3/ψ_3) fragments (Figure 5A)
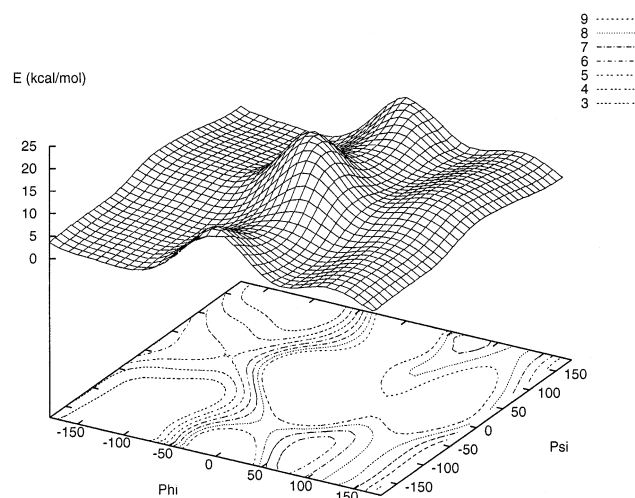
Figure 4. Dihedral energy surfaces for the dipeptide: the total energy of the fragment is plotted against dihedral values as a 3D plot (upper plots) and as a contour plot (lower plots). Energies of the contour plots are given in the legend.

are characterized by six well-defined minima. Comparison of the CPCT map with the DIPEP map reveals a maximum at (ϕ_3

$= -120$, all ψ_3) in the former; this ridge arises from steric repulsions between the hydroxyl group and the central methyl group of the CPCT and separates the large minimum ($\phi = -60$ to $\phi = -180$) of the standard Ramachandran plot into two sets of minima near $\phi = -60$ and $\phi = -180$, see Figure 7. Corresponding behavior is found in the ϕ_1/ψ_1 map. The map for the central portion of the cis-enediol analogue (CPCIS) is very different from the DIPEP map (compare α/β and ϕ/ψ maps in Figures 5A and 4). There are two equivalent low energy regions with minima at ($\alpha = -100$, all β) and ($\beta = 100$, all α) and a large excluded region for ($-50 < \alpha < 180$) and ($-180 < \beta < 50$). Maps for the other stereoisomers are very similar, with small changes of the relative values of the extrema but not of their locations. By contrast, the α/β map for the CPTRANS configuration (data not shown) shows only weak extrema, and all α/β values are accessible, indicating that the CPTRANS configuration is significantly less sterically constrained than the CPCIS configuration.

3.2.2. Grid Scan. The $6^6 = 46\,656$ conformations obtained from the grid-scan procedure (see section 2.2.1) for each of the stereoisomers were clustered according to their dihedral angle values using a radius of 30°. The distribution of the resulting
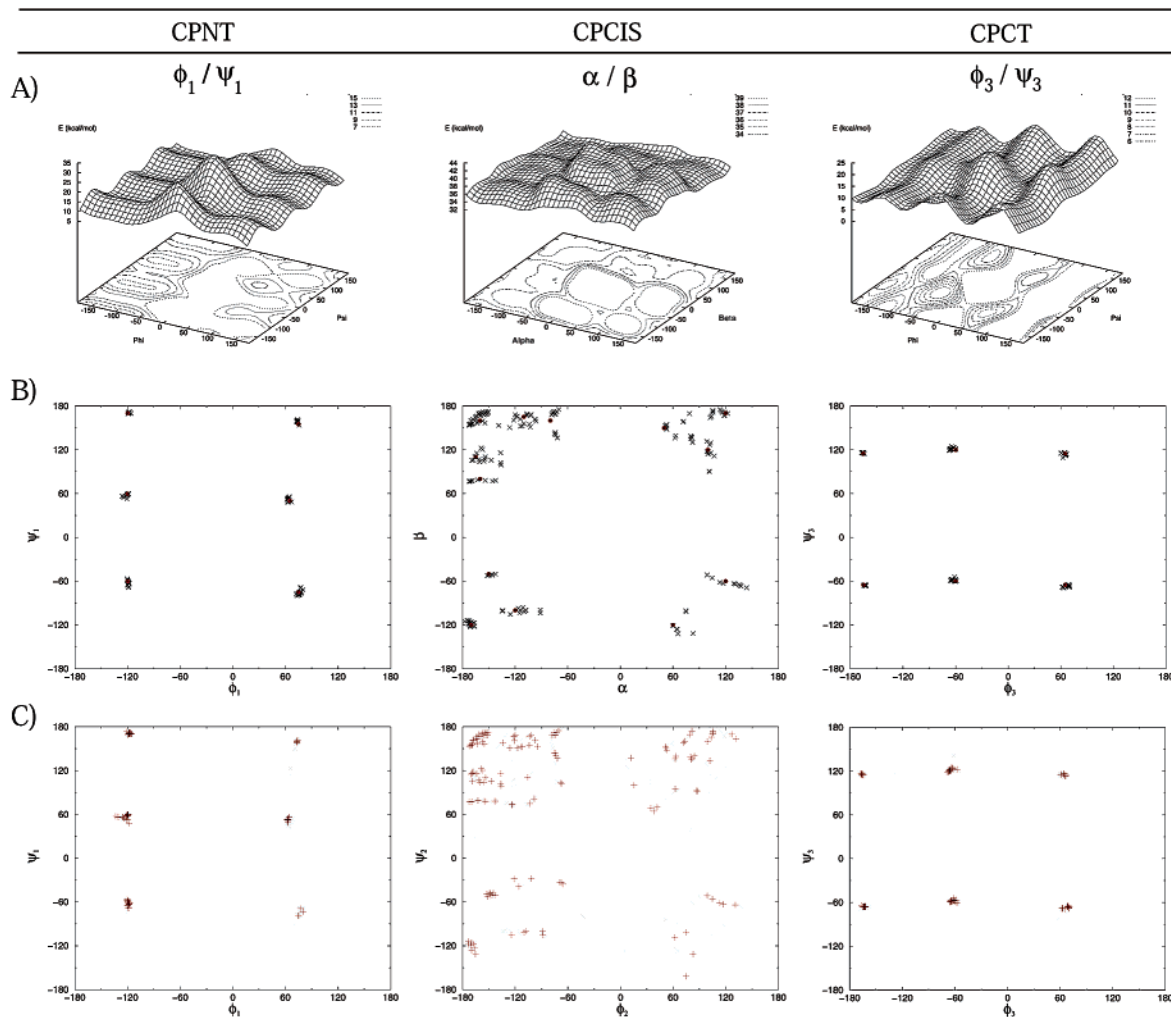

Figure 5. Example of results of the methods used to analyze the conformational space. The results are for the SRSR stereoisomer and trialanine at $\epsilon = 80$. (A) Dihedral energy surfaces for the three CPEP fragments: the total energy of the fragment is plotted against dihedral values as a 3D plot (upper plots) and as a contour plot (lower plots). (B) Build-up: Values of the dihedrals obtained after building all possible combinations using the chosen minima of the fragment energy surface (see text); the minima of the map used for reconstruction are shown by red dots in (B) for the SRSR CPEP. (C) Grid scan: Values of the ϕ_1/ψ_1, α/β, and ϕ_3/ψ_3 dihedral angles for all clusters (gray marks) and for the cluster selected for the database (red marks).
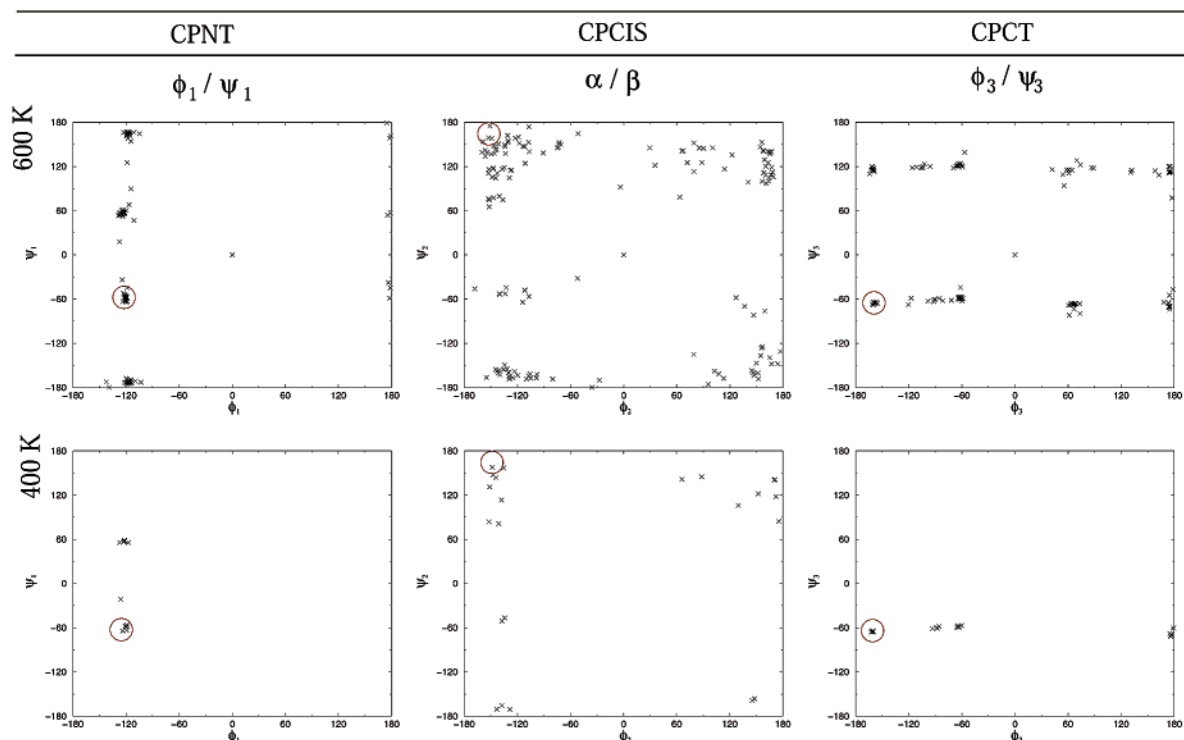
Figure 6. Molecular dynamics results: Values of the ϕ_1/ψ_1, α/β, and ϕ_3/ψ_3 dihedral angles for all clusters obtained from the 600 K/400 K MD runs. The red circles indicate the starting geometry.
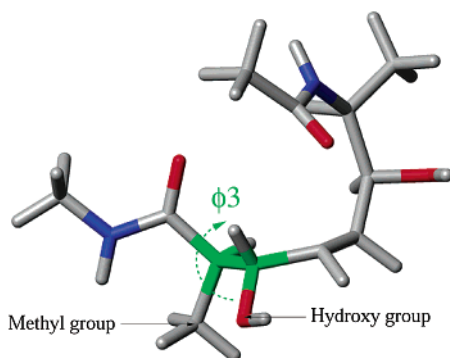

Figure 7. Origin of the additional ridge on the ϕ_3/ψ_3 energy surface at $\phi_3 \approx -120$. This dihedral value results in an alignment of the methyl group and the hydroxy group that creates a steric repulsion. A distance of 2.6 Å between the two groups was found for this conformation after minimization, with a van der Waals interaction energy of $+1.38$ kcal/mol. The bonds defining the ϕ_3 dihedral angle are shown in green.

clusters according to their size and their energy (defined as the energy of the conformer whose dihedral angle values are the closest to the average values over the cluster, see section 2.2.1) is shown in Figure 3A for all of the stereoisomers. The clusters obtained by a similar grid-scan procedure for DIALA and TRIALA are shown in Figure 3B and C, respectively. Because the grid-scan procedure produced 17 and 125 clusters for DIALA and TRIALA, respectively, all clusters were included in the database. The small number of clusters found for DIALA is due to the presence of only four free dihedral angles as compared to six for TRIALA and CPEP.

The ϕ/ψ values obtained by the grid-scan procedure are shown in Figure 5C; the red marks indicate clusters that were included in the database. Each minimum of the energy surface corresponds to a well-populated region from the grid-scan method, and all of the maxima correspond to an excluded region.

There are six well-defined preferential regions of the ϕ_1/ψ_1 and ϕ_3/ψ_3 planes that contain all of the minima. The conformations included in the database (red marks) occupy all six regions. The α/β plane is characterized by important regions of exclusion around values of $(0,0)$, $(0,-150)$, $(150,0)$, and $(120,-120)$, corresponding to maxima of the dihedral energy surface (see section 3.2.1). These results show the good correspondence between the minima/maxima of the dihedral energy surface and the spanned/excluded regions of the grid-scan method which provides an essentially complete sampling of the dihedral angle space. The conformers of the grid database (red marks) also include all of the important minima of the energy surface.

3.2.3. Reconstruction from Dihedral Angle Energy Surfaces. Starting with six preferred regions for the ϕ_1/ψ_1 surface, $(-120,-60)$, $(-120,60)$, $(-120,170)$, $(75,-75)$, $(60,65)$, and $(75,165)$, four for the ϕ_2/ψ_2, $(-120,-60)$, $(-120,120)$, $(60,120)$, and $(120,-120)$, and six for the ϕ_3/ψ_3, $(-165,-65)$, $(-165,115)$, $(-60,-60)$, $(-60,120)$, $(65,-65)$, and $(65,115)$, we obtained the 144 possible conformers after minimization (see section 2.2.2), and they are shown in Figure 5B. They were compared to the clusters in the grid database with a tolerance of 15° for ϕ_1/ψ_1 and ϕ_3/ψ_3 and 60° (to reflect the broader minimum energy regions) for α/β. Some combinations of dihedrals that were not found in the grid database like $\phi_1/\psi_1 = (75,165)$, $\phi_2/\psi_2 = (60,120)$, $\phi_3/\psi_3 = (-60,120)$, for example, correspond to backbone clashes. On average, 50.0% of the 144 possible combinations corresponded to impossible geometries. Overall, the build-up procedure minima matched 75% of the 150 clusters obtained from the grid-scan procedure. All 12 lowest energy clusters (between 0 and 2.21 kcal/mol; energies are given relative to the lowest energy conformer) are exactly reproduced (i.e., the same conformer is found after minimization), and among the 50 lowest energy clusters (between 0 and 4.16 kcal/

mol), all but 14 are exactly reproduced. The 25% of the minima that were not reproduced are minor minima of the α/β map; they correspond to an expansion of the allowed regions for α/β as can be seen by a comparison of Figure 5B and C.

The build-up method is much less computation intensive because only 144 conformations are minimized as compared with $6^6 = 46\,656$ conformations for the grid-scan procedure. There is a reduction of a factor of about 300 here, and the factor would be even greater for larger peptides. Thus, the present comparison between a full grid search and the build-up procedure supports the use of the latter for more complicated systems.

3.2.4. Molecular Dynamics. Three vacuum MD simulations were performed at 400, 500, and 600 K as described in section 2.2.3. The resulting trajectories were clustered using the values of the dihedral angles as done for the grid-scan minima. The 600 K run resulted in 153 clusters, the 500 K run resulted in 65, and the 400 K run resulted in 24 clusters. The resulting dihedral angle maps, for the 400 and 600 K MD, are compared to those from the grid-scan method in Figures 5C and 6. The dynamics result in clusters similar to the ones found by the grid scan method. However, many of the clusters found in the grid scan method are not sampled, even in the 600 K MD run. The situation is worse for the lower temperature MD runs. For example, starting from the $\phi_1/\psi_1 = (-120.05, -58.55)$, $\phi_2/\psi_2 = (-159.42, 166.57)$, and $\phi_3/\psi_3 = (-162.97, -65.69)$ minimum found in the grid-scan method (cluster of energy 38.215 kcal/mol and population of 403 members, red dots in Figure 6), only the minima at $\psi_3 \approx -60$ are sampled at 400 and 500 K. It required the 600 K run to sample the other minima at $\psi_3 \approx +120$. For the ϕ_1/ψ_1 plane, the minima on the line $\phi_1 \approx -120$ are already populated in the 400 and 500 K runs, but the minima on the line $\phi_1 \approx +60$ are never reached even with the 600 K run. This indicates that the free energy barriers between the minima along the $\phi_1 \approx -120$ are lower than those along the $\phi_1 \approx +60$ line. The result is consistent with the energy surface for the corresponding fragments (see Figure 5A). The central dihedral map (α/β) is also only partially populated at 400 and 500 K, but the 600 K simulation provides a good sampling. Overall, the 400 K MD simulation reproduced 10% of the grid scan database minima, the 500 K simulation reproduced 12%, and the 600 K simulation reproduced 38%, using the same tolerances as described in paragraph 3.2.3 for the dihedral angles.

The computation times required for the dynamics runs are comparable to those of the grid-scan method. Thus, the latter provides a much more thorough exploration of the conformational space than the former for the same computational cost. In addition, the grid-scan method is easily and efficiently parallelized.

3.3. Comparison of CPEP with Alanine Di- and Tripeptides. For all 124 TRIALA (energy from 0 to 12.59 kcal/mol relative to the minimum) and 17 DIALA (energy from 0 to 19.47 kcal/mol relative to the minimum) clusters, one or more CPEP clusters were found within an RMSD < 1 Å, using the correspondence of atoms in Figure 1A; the RMSD values ranged from 0.37 to 0.78 Å for DIALA and from 0.52 to 0.93 Å for TRIALA, although higher energies may be involved in CPEP versus DIALA/TRIALA. For the 28 TRIALA conformers with energies below 2 kcal/mol, the range of energies of CPEP required for a 1 Å RMSD is 0.0–2.21 kcal/mol; correspond-
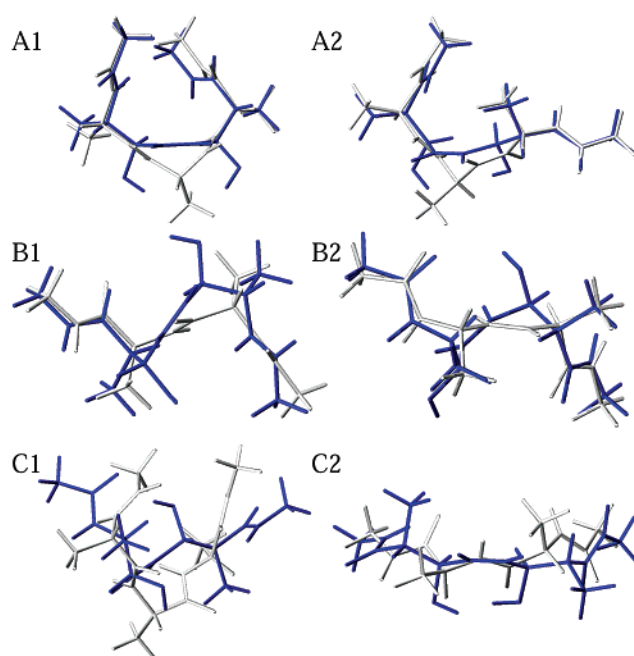
Figure 8. Comparison of low-energy minima. The TRIALA and DIALA structures are shown in light gray, and the CPEP are shown in blue. (A) TRIALA comparison: (A1) CPEP SRSR stereoisomer with an RMSD of 0.57 Å. The energies relative to the lowest energy conformer are 0.0 and 0.49 kcal/mol for the CPEP and TRIALA, respectively. (A2) CPEP SSRR stereoisomer with an RMSD of 0.57 Å. The energies relative to the lowest energy conformer are 1.31 and 0.95 kcal/mol for the CPEP and TRIALA, respectively. (B) DIALA comparison: (B1) CPEP SRSR stereoisomer with an RMSD of 0.61 Å. The energies relative to the lowest energy conformer are 2.92 and 3.93 kcal/mol for the CPEP and DIALA, respectively. (B2) CPEP SSRS stereoisomer with an RMSD of 0.39 Å. The energies relative to the lowest energy conformer are 2.39 and 0.0 kcal/mol for the CPEP and DIALA, respectively. (C) CPEP conformations without close DIALA/TRIALA correspondent: (C1) CPEP SRSS stereoisomer with an RMSD of 1.96 Å. The energies relative to the lowest energy conformer are 1.65 and 0.0 kcal/mol for the CPEP and TRIALA, respectively. (C2) CPEP RSRR stereoisomer with an RMSD of 2.09 Å. The energies relative to the lowest energy conformer are 0.74 and 0.30 kcal/mol for the CPEP and DIALA, respectively.

ingly, for the seven DIALA conformers with energies below 2 kcal/mol, the range of energies of CPEP required for a 1 Å RMSD is 0.27–1.85 kcal/mol. Figure 8A and B makes clear that the methyl "side chains" can have corresponding orientations in the cis-enediol unit and the peptides.

Table 2 gives the percentage of TRIALA minima that are matched by each stereoisomer within certain RMSD tolerances. As can be seen, the coverage is excellent and essentially complete for an RMSD of 1.2 Å. It is striking, although not unexpected, that for a given pair of enantiomers, their ability to mimic the asymmetrical peptide molecules is very different; for an RMSD cutoff of 1.0 Å, important differences are seen between the different stereoisomers, with a percentage of 88% for the SRSR stereoisomer as compared to 35% for its enantiomer, RSRS. Table 3 lists the percentage of the 17 DIALA and 150 TRIALA minima that are best matched (lowest RMSD) by a given CPEP stereoisomer. Again, a strong dependence on the stereoisomer is observed. The SRSR stereoisomer is most frequently found (23%) to match TRIALA, and RSSR is most frequently found (29%) to match DIALA.

A histogram of the RMSD values obtained after optimal superposition of each of the conformers of selected CPEP
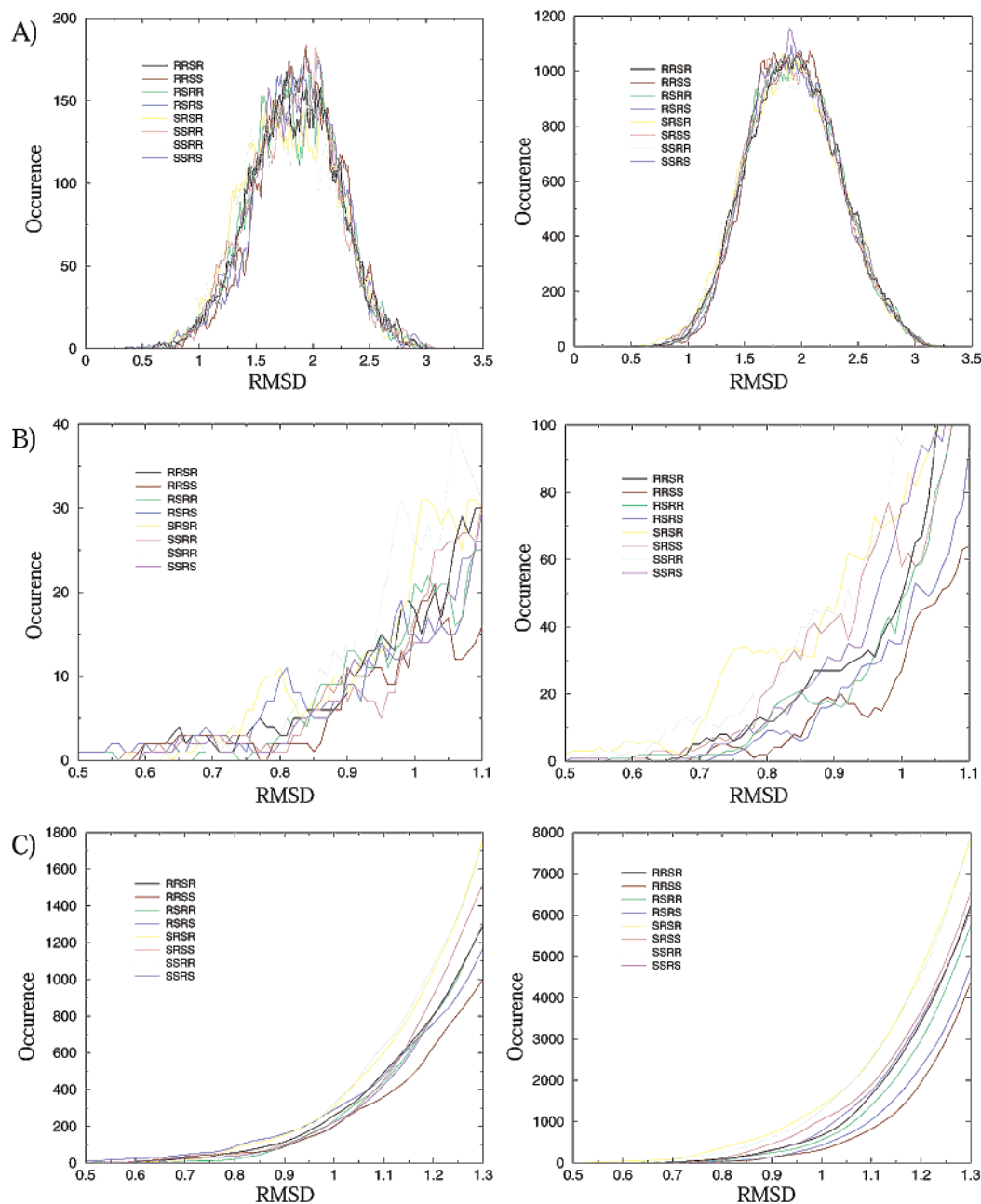
Figure 9. RMSD (in Å) distributions for selected CPEP stereoisomers in comparison with the DIALA (left panels) and the TRIALA (right panels). (A) Entire distributions. (B) Blowup of the low RMSD region of the entire distribution. (C) Cumulated number of structures computed from the curves of (B) (see text).

stereoisomers with each DIALA and TRIALA conformer (using the atom correspondence of Figure 1) is shown in Figure 9A. The distributions are similar for all of the stereoisomers, although there are substantial variations for the lower RMSD values that are presented in Figure 9B. The cumulated sum is given in Figure 9C. The SRSR and the SSRR stereoisomers have significantly larger populations at low RMSD values relative to both DIALA and TRIALA. In the TRIALA comparison, those two stereoisomers are always much more represented than the others. For example, the number of structures having an RMSD lower than 0.6 Å is 40 for the SRSR stereoisomer and 20 for the SSRR stereoisomer, as compared to 5 for the next most represented stereoisomer (SSRS, see Figure 3C). The situation is similar for the DIALA comparison, although the differences are not as pronounced. Because the

number of DIALA clusters is much smaller (17 as compared to 125), the statistics for the low RMSD values are not very reliable. Nevertheless, the SRSR and SSRR stereoisomers are predominant in the cumulative distribution for values greater than 1.0 Å. For less than 1.0 Å, the SRSR stereoisomer is always dominant; another stereoisomer, RSRS, is also important. Again, the part of the curve for RMSD < 1.0 Å suffers from the poor statistics. Interestingly, the trend observed at low RMSD values is also observed for the entire distribution. The complete RMSD distributions (see Figure 3A) were fitted by Gaussian curves, and the resulting average (μ) and standard deviations (σ) are given in Table 4. For both DIALA and TRIALA, the mean of the distribution is lowest for the SRSR and SSRR stereoisomers. For TRIALA, another stereoisomer, SRSS, also has a lower mean than the other stereoisomers. Because the distributions

are not significantly different for RMSD > 2 Å, the differences are due to the low RMSD part of the curves (i.e., RMSD < 2.0 Å).

Importantly, there exist CPEP conformers that are quite different from those of natural peptides. If one considers the 282 structures of CPEP and the 28 of TRIALA within 2 kcal/mol of the lowest energy conformers for all of the stereoisomers, there are 76 CPEP conformers that *cannot* be matched within an RMSD less than 1.5 Å (up to 1.96 Å in the worst case). A similar result is found for the 7 DIALA structures: within 2 kcal/mol from the lowest energy conformer, 147 CPEP conformers cannot be matched with an RMSD less than 1.5 Å (see Figure 8C).

3.4. Comparison with Experimental Results. The IC_{50}'s, in μM, of the 32 compounds are given in Table 5. The activities range over at least 2 orders of magnitude, from 10 to >1000 μM. It is clear that there is a strong influence of the stereochemistry of the four asymmetrical carbons of the cis-enediol unit on the activity of the compounds. For compounds of the $(i, i + 1)$ series with the first chiral center having an R configuration, the IC_{50} values range from 168 to 1130 μM. By contrast, $(i, i + 1)$ compounds having an S configuration for the first chiral center exhibit an IC_{50} ranging from 10.2 to 46.6 μM, with the exception of the SRSS compounds which have an IC_{50} of 215 μM. The most active compounds, with IC_{50} lower than 50 μM, have an S configuration at the first chiral center, which corresponds to the natural stereoisomer of leucine, that is, L-Leu. The second chiral center can present either an S or an R configuration. There is no restriction on the third and fourth positions in the $(i, i + 1)$ series, but there is a preference for RR in the $(i, i + 2)$ series. The best compounds against renin in this library exhibit an approximately 40-fold improvement in potency as compared to the unmodified angiotensinogen peptide, which has an IC_{50} of 400 μM (see section 2.2.4 for details).

The experimental results can be compared with the percentage of TRIALA minima that are matched by each "ALA-ALA" peptide analogue stereoisomer with an RMSD tolerance of 1.1 Å. It varies from 52.85 to 83.74% for RXXX "ALA-ALA" to 81.30 to 96.75% for SXXX "ALA-ALA". The cis-enediol unit stereoisomers that have the strongest activity toward renin are the ones that were shown here to be best able to match the conformations of natural peptides. Moreover, a rather good correlation was found between the IC_{50} of $(i, i + 1)$ compounds and the ability of the corresponding "ALA-ALA" peptide analogue to match the conformation of TRIALA minima with a RMSD tolerance of 1.1 (%matched):

$$pIC_{50} = 6.1 - 0.05\%\,matched$$

$$R = 0.7683, \quad \sigma = 0.55, \quad Q = 0.7135$$

where $pIC_{50} = -\log(IC_{50})$, R is the correlation coefficient, σ is the standard deviation, and Q is the correlation coefficient obtained by the "leave one out" method. To derive this equation, IC_{50} values that were not determined, but were larger than 1000 μM, were set equal to 1000 μM. The "leave one out" method is a cross-validation procedure that systematically removes one point at a time from the data set. A model is then derived using the remainder of the data and is subsequently used to predict a value for the point left out, which can be compared with the

observed value. This is repeated for every point in the data set and permits the calculation of a cross-validated correlation coefficient.[9] The cross-validated correlation coefficient is a measure of the goodness of prediction.

Despite the simplicity of the approach, this QSAR equation is able to explain 59% (R^2) of the variability of the activity of the compounds toward renin. This suggests that the activity of the $(i, i + 1)$ peptide analogues against renin is correlated with their ability to mimic native peptide conformations (i.e., to reproduce similar interactions with their environment) as evaluated by the modeling studies.

Similar observations apply to the $(i, i + 2)$ series. As was already observed for this series, an RR configuration for the third and fourth chiral centers, for peptide analogues having an S configuration for the first chiral center, seems to promote a stronger activity against renin. Table 5 shows that, similarly, the highest fractions of TRIALA minima that are matched by a given "ALA-ALA" peptide analogue stereoisomer with a RMSD tolerance of 1.1 Å are encountered for SXXR compounds: 90.24, 95.12, 90.24, and 96.75 for SRRR, SRSR, SSRR, and SSSR "ALA-ALA", respectively. No compounds having a cis-enediol unit that badly reproduce regular peptide conformational space appear to have a large activity toward renin. However, compounds having a low activity toward renin but also having a cis-enediol unit able to reproduce well the conformational space of TRIALA were found, such as the $(i, i + 2)$ SRSR peptide analogues. Thus, it seems that the ability of the cis-enediol unit to reproduce the conformational space of TRIALA, as evaluated by the conformational analysis, is a necessary but not sufficient condition for a large activity in the renin test.

4. Concluding Discussion

A study has been made of the conformation space accessible to a set of cis-enediol peptide analogues. Comparison of the grid search method in the full dihedral angle space with a build-up procedure showed good agreement. The grid search yields a more thorough exploration of the conformation space, but it is more demanding in CPU resources. The ϕ/ψ energy surface build-up method is much faster (with a 300-fold reduction in computational time for the present system) and provides essentially complete sampling of the conformational space of the cis-enediol unit; corresponding results are obtained in the di- and tripeptide searches. The comparison of the two methods for this case, where both are feasible, supports the use of the build-up procedure in larger systems. The MD simulations, even at high temperature (600 K), explored only part of the conformational space. However, such simulations can provide useful information on the free energy barriers between the minima.[10] It is then possible to draw a map of the connected minima at a given temperature which might be useful when deciding which conformations to include in a docking algorithm, for example. This information is not obtained by the grid-scan method, as used here.

The different stereoisomers of the cis-enediol unit have a wide spectrum of conformations, some very close to natural di- and tripeptides and others that are distinct from them. By contrast,

(9) Leach, A. R. *Molecular Modeling*, 2nd ed.; Pearson Education: Harlow, England, 2001; Chapter 12, p 701.
(10) Becker, O. M.; Karplus, M. *J. Chem. Phys.* **1997**, *106*, 1495−1517.

all of the minima of the di- or the trialanine peptide could be matched closely by minima of one or more of the stereoisomers in the peptide analogue database. Some of the stereoisomers, SRSR and SSRR, in particular, are more frequently found as the best stereoisomers to match minima of TRIALA. Comparison of the ability of each stereoisomer to match DIALA or TRIALA with its activity in a renin inhibition study showed a good correlation, indicating that the peptidomimetic potential of the different stereoisomers can be evaluated by the present molecular modeling approach. This suggests that, in practice, the selection of the best stereoisomer to use will be facilitated by performing a systematic superposition with the natural peptides if one is trying to mimic a known peptide inhibitor. Alternatively, one may use the analysis to pick a subset of stereoisomers that best cover certain regions of conformational space.

Supporting Information Available: Atomic charges of the CPEP molecule; database containing the 150 selected cluster centers for each stereoisomer (pdb files). This material is available free of charge via the Internet at http://pubs.acs.org.

JA012695P